Numerical Investigation of Ultrasonic Wave Propagation in Tapered Waveguides

R. Kažys[1], R. Rekuvienė[1], E. Žukauskas[1]
[1]*Ultrasound Institute, Kaunas University of Technology,*
Studentu St. 50, LT-51368 Kaunas, Lithuania
ui@ktu.lt

***Abstract*—Ultrasonic transducers are used for in-line, non-intrusive and non-destructive process monitoring of molten metals, liquids and other materials at elevated temperatures. In this case special high temperature waveguides must be used to protect the surface of the transducer from influence of a high temperature. Objective of this work was numerical investigation of ultrasonic wave propagation in tapered waveguides with *λ*/4 impedance matching layers of finite lateral dimensions.**

***Index Terms*—Ultrasonic measurements, ultrasonic waveguides, 3D modelling, 2D modelling.**

I. INTRODUCTION

Ultrasonic techniques are widely used for non-destructive testing of metallic structures, characterization of different material properties and process control [1]. The advantages of ultrasonic methods are high speed of measurements what enables to use them for on-line measurements and monitoring of manufacturing processes [2]. In some cases ultrasonic methods may be applied for investigation of properties materials in extreme conditions, for example of hot fluids, melted metals at high pressures and high temperatures [3]. In order to protect piezoelectric transducers from influence of a high temperature and/or pressure ultrasonic waves are transmitted via solid waveguides usually of a circular cross-section [4]–[6].

Literature analysis and our previous works revealed that in cylindrical waveguides trailing waves are generated, which in most cases complicate and reduce accuracy of ultrasonic measurements [4], [7]. The appropriate selection of a geometric shape and material of the waveguide selection is very important in order to increase reliability of measurements. One of simple and efficient ways to reduce trailing echoes is application of tapered waveguides (Fig. 1) [8].

In order to achieve efficient wave transmission from a waveguide to liquid under investigation additional layers for impedance matching may be used. On the other hand some measurements may be performed in a pulse- echo mode in which the ultrasonic pulses reflected from the interface waveguide tip- medium under investigation are analysed. In the latter case performance of the tapered waveguide with the *λ*/4 matching layer (is the *λ* wavelength) of finite lateral dimensions becomes very important. To our knowledge detailed analysis of propagation of ultrasonic pulse wave in such structures is still missing. [6].

Objective of this work was numerical investigation of ultrasonic wave propagation in tapered waveguides with *λ*/4 impedance matching layers of finite lateral dimensions using two different modelling techniques: 2D finite element and 3D finite difference (Wave 3000) techniques.

II. MODELS OF THE ULTRASONIC WAVE PROPAGATION IN THE WAVEGUIDES

Numerical modelling of the ultrasonic wave propagation in the tapered waveguide was carried out using 3D finite difference (FDM) and 2D finite element techniques (FEM). Graphical representation of the model used in 3D finite difference technique (Wave 3000) is presented in Fig. 1.

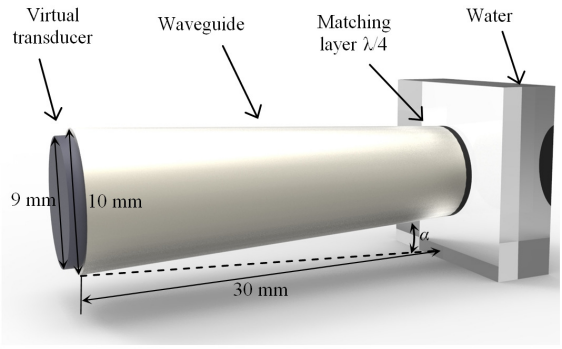

Fig. 1. 3D model of the tapered waveguide.

The visco-elastic wave equation solved by 3D finite difference technique (Wave 3000) is the following [9]

$$\rho\frac{\partial^2 w}{\partial t^2}=\left(\mu+\eta\frac{\partial}{\partial t}\right)\nabla^2 w+\left(\lambda+\mu+\xi\frac{\partial}{\partial t}+\frac{\eta}{3}\frac{\partial}{\partial t}\right)\nabla(\nabla\bullet w), \quad (1)$$

where $w = w(x, y, z, t)$ is the displacement vector, which is function of coordinates x,y,z and time t, λ and μ are the Lame constants, ρ is the density, η and ξ are the shear and bulk viscosity.

The length of the modelled waveguide was 30 mm. The diameter of the waveguide front surface, contacting with the ultrasonic transducer was 10 mm. The angle α was selected 2.3^0. The diameter of the virtual ultrasonic transducer was 9 mm. Generation and reception of ultrasonic waves in the

Manuscript received January 25, 2013; accepted April 5, 2013.

model is performed by so called virtual transducers which are transparent for ultrasonic waves and do not cause any reflections. Modelling of the ultrasonic wave propagation was performed for two materials - titanium and steel. In both cases $\lambda/4$ layers were used for matching materials with different acoustic impedances in order to achieve more efficient transmission of the ultrasonic wave through the waveguide-fluid interface [6]. In the case of the titanium waveguide the matching layer made of PBI (polybenzimidazol) was used. The thickness of matching layer was 0.21 mm. In the case of the steel waveguide the matching layer is made of a special aluminium alloy. In this case the thickness of the matching layer was 0.34 mm. The material properties used in the modelling are presented in Table I.

TABLE I. MATERIAL PROPERTIES.

	Density, kg/m^3	Longitudinal velocity, m/s	Shear velocity, m/s
Titanium	4480	6100	3100
Steel (AISI 316)	7990	5577	3068
PBI	1296	2970	1460
Aluminium alloy	2200	4700	2820
Water	1000	1480	-

The virtual ultrasonic transducer operating in a pulse echo mode was placed on the wide end on the waveguide. The radius of the transducer was 4.5 mm. The virtual ultrasonic transducer generated a normal displacement. For excitation of the ultrasonic wave in the waveguide the 3.5 MHz, 3 periods sine burst with the Gaussian envelope was used.

Modelling of the ultrasonic wave propagation in the waveguides was carried out using a finite element technique as well. The modelling was performed using the finite element software ANSYS. Because the finite element technique requires huge computational resources, the finite element model was simplified using an axial symmetry approach. Graphical representation of the finite element model is presented in Fig. 2.

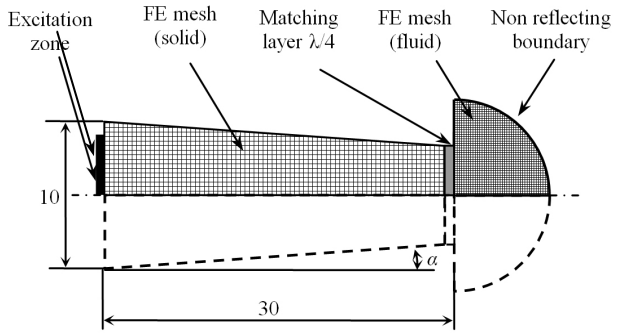

Fig. 2. Graphical representation of the 2D finite element model.

The following dynamic equation was solved

$$[\mathbf{M}]\{\ddot{\mathbf{U}}\}+[\mathbf{C}]\{\dot{\mathbf{U}}\}+[\mathbf{K}]\{\mathbf{U}\}=\{\mathbf{F}(t)\}, \quad (2)$$

where [**M**] is the structural mass matrix, [**C**] is the element damping matrix, [**K**] is the structural stiffness matrix, {**U**} is the displacement vector, {**F**} is the structural load vector. The material properties used in the FE modelling are presented in Table I. The solid domain (waveguide and matching layer) of the model was meshed using PLANE42 elements and the fluid domain was meshed using FLUID29. The spatial resolution of the mesh is $\lambda_l/30$ for solid domain and $\lambda_l/20$ for fluid domain (λ_l is length of the longitudinal wave). Non - reflecting boundary conditions on the fluid domain boundaries were used in order to avoid reflections of the ultrasonic waves. For excitation of the ultrasonic wave 3.5 MHz sine burst with Gaussian envelope was used.

III. RESULTS ANALYSIS

In Fig. 3 and Fig. 4 the displacement fields of the ultrasonic wave propagating in the tapered waveguide at different instants of time are presented. In Fig. 3 displacement fields in the titanium waveguide with PBI matching layer and in Fig. 4 in the tapered steel waveguide with the aluminium matching layer are shown. Spatial distributions of the displacement fields are presented in $y0z$ (Fig. 3(a, b, c, d) and Fig. 4(a, b, c, d)) and in $x0y$ (Fig. 3(e, f, g, h) and Fig. 4(e, f, g, h)) cross-sections of the waveguide.

A complex combination of displacement fields is observed (Fig. 3 and Fig. 4). At first a longitudinal ultrasonic wave (L) is propagating. This wave is reflected by the cylindrical surfaces of the waveguide. The reflected waves propagate to the centre of the waveguide (Fig. 3(a, e) and Fig. 4(a, e)) where interference of the waves occurs. The waves travelling behind the longitudinal wave are so- called trailing waves. Such signals are unwanted, because they can overlap with the wave of the interest and cause the measurement uncertainty. At the solid - liquid interface reflection and transmission of the ultrasonic wave occur and part of the wave is travelling back to the ultrasonic transducer (Fig. 3(c, d) and Fig. 4(c, d)). The displacement fields in transversal cross-sections presented in Fig. 3 (g, h) and Fig. 4 (g, h) show a non-uniform structure of the fields which are distorted by overlapping pulse waves.

Time diagrams of the transmitted and reflected signals in a case of titanium waveguide obtained using the finite difference and finite element techniques are presented in Fig. 5. The results obtained with 3D finite difference technique and 2D axisymmetric finite element technique are very similar. Frequency characteristics of reflection and transmission coefficients obtained from modelling results are shown in Fig. 6. In order to reveal advantage and gain of the $\lambda/4$ matching layer all characteristics were normalised according to the maximum of the value of the curve obtained in a case of the waveguide without a matching layer. Fig. 6(a) shows that in the case of the waveguide with a matching layer there is minimum of the reflection coefficient near 3,5 MHz frequency for which the thickness of the matching layer was selected. In this frequency zone the reflection coefficient is about 2 times smaller than in the case of the waveguide without the $\lambda/4$ matching layer. Efficiency of the transmission of the ultrasonic wave through the waveguide - water interface can be presented as the transmission coefficient (Fig. 6(b)). The obtained results show that in case of the waveguide with the $\lambda/4$ matching layer the transmission coefficient is two times bigger than in the case of the waveguide without a matching layer.

The time diagrams of the received signals in a case of a

steel waveguide are presented in Fig. 7. The signals in this case are slightly different than in the titanium waveguide case, but regularities of the transmission and reflection of the ultrasonic wave are the same.

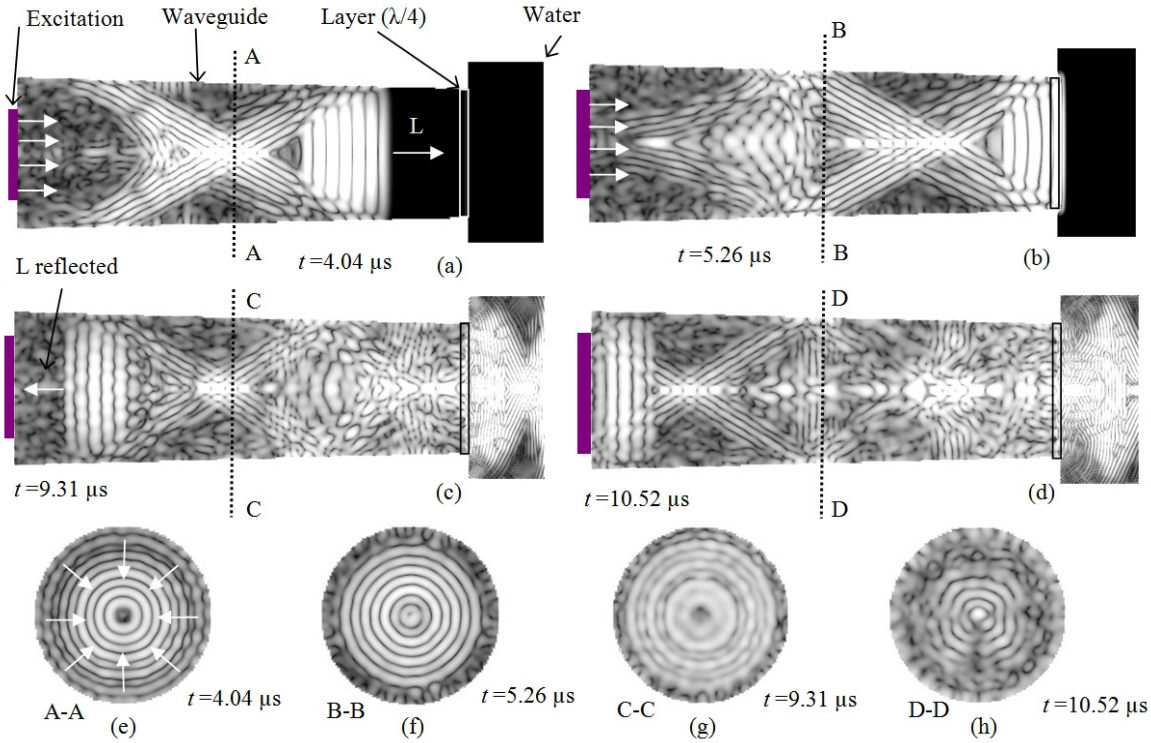

Fig. 3. Displacement fields of the ultrasonic wave propagating in the tapered titanium waveguide with PBI matching layers at the different instants of time: a, b, c, d – *y*0*z* cross-section, e, f, g, h – *x*0*y* cross-section.

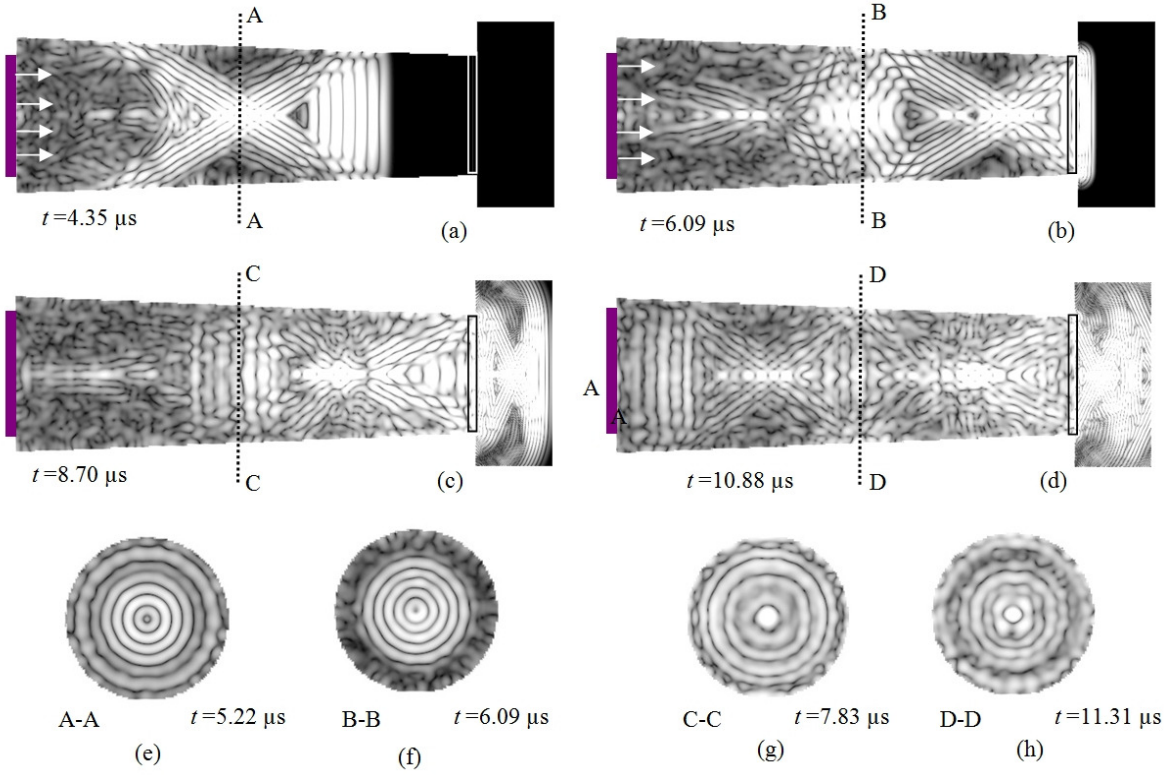

Fig. 4. Displacement fields of the ultrasonic wave propagating in the tapered steel waveguide with aluminium matching layers at the different instants of time: a, b, c, d – *y*0*z* cross-section, e, f, g, h – *x*0*y* cross-section.

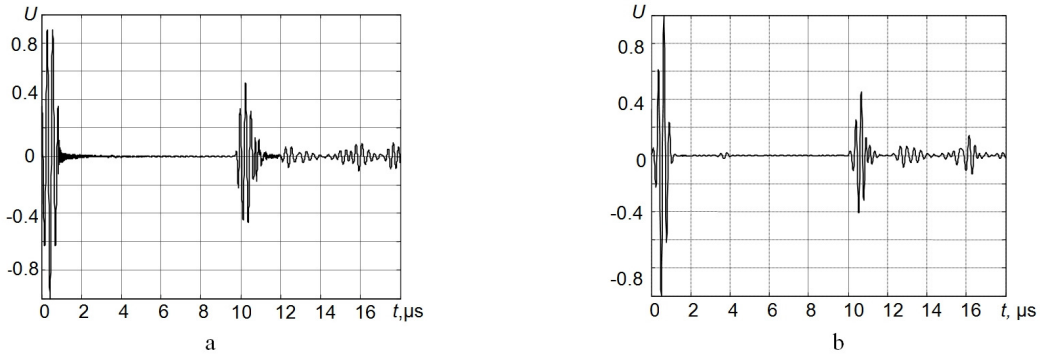

Fig. 5. Time diagrams of the modelled signals reflected by the interface waveguide/liquid and received by the ultrasonic transducer in a case of 2,3° tapered titanium waveguide. a – 3D finite difference technique (Wave 3000), b – 2D finite element technique (ANSYS).

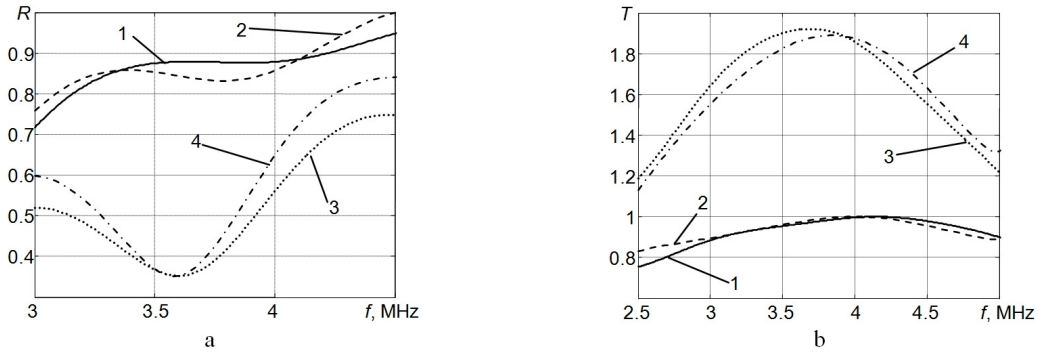

Fig. 6. Normalised reflection coefficient from interface between waveguide and water in a case of titanium waveguide: 1 – waveguide without matching layer (FEM), 2 – waveguide without matching layer (FDM), 3 – waveguide with matching layer (FEM), 4 – waveguide with matching layer (FDM).

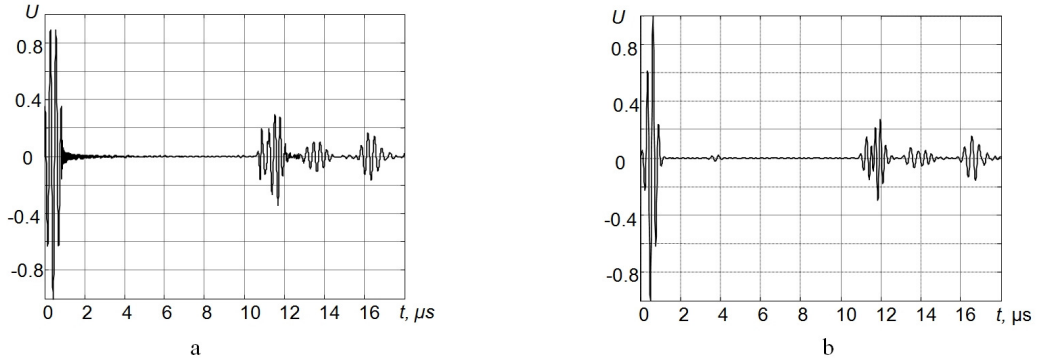

Fig. 7. Time diagrams of the modelled signals reflected by the interface waveguide/liquid and received by the ultrasonic transducer in a case of 2,3° tapered stainless steel waveguide: a – 3D finite difference technique (Wave 3000); b - 2D finite element technique (ANSYS).

IV. CONCLUSIONS

Numerical modelling of ultrasonic wave propagation in titanium and steel waveguides revealed a very complicated character of the propagating wave. The "tail" of the propagating wave remains even if a tapered waveguide is used. It may influence accuracy of measurements especially in a pulse- echo mode. Nevertheless, application of the $\lambda/4$ matching layer improves matching of the acoustic impedances of the waveguide and the medium under investigation and consequently the transmission coefficient increases up to two times.

REFERENCES

[1] M. Kobayashi, C.-K. Jen, J. F .Bussiere, K.-T. Wu, "High-temperature integrated and flexible ultrasonic transducers for non-destructive testing", *NDT&E International*, vol. 42, pp. 157–161, 2009. [Online]. Available: http://dx.doi.org/10.1016/j.ndteint.2008.11.003

[2] C. Jen, J. Legoux, L. Parent, "Experimental evaluation of clad metallic buffer rods for high temperature ultrasonic measurements", *NDT&E International*, vol. 33, pp. 145–153, 2000. [Online]. Available: http://dx.doi.org/10.1016/S0963-8695(99)00042-0

[3] C. Jen, K. Nguyen, J. Legoux, I. Ihara, H. Hebert. "Novel clad ultrasonic buffer rods for the monitoring of industrial materials processing", *NDT&E International*, vol. 4, pp. 1–6, 1999.

[4] R. Kažys, E. Žukauskas, R. Rekuvienė, "Modelling of ultrasonic measurement systems with waveguides", *Elektronika ir Elektrotechnika (Electronics and Electrical Engineering), no.* 7, pp. 61–64, 2012.

[5] R. Kažys, A. Voleišis, R. Šliteris, B. Voleišienė, L. Mažeika, "Development of ultrasonic sensors for operation in as heavy liquid metal", *IEEE Sensors Journal*, vol. 6, pp. 525–537, 2006. [Online]. Available: http://dx.doi.org/10.1109/JSEN.2006.877997

[6] R. Kažys, A. Voleišis, R. Šliteris, L. Mažeika, "High temperature ultrasonic transducers for imaging and measurements in a liquid Pb/Bi eutectic alloy", *IEEE Transactions on Ultrasonics, Ferroelectrics, and Frequency Control*, vol. 52, pp. 525–537, 2005. [Online]. Available: http://dx.doi.org/10.1109/TUFFC.2005.1428033

[7] R. Thurston, "Elastic waves in rods and clad rods", *J. Acoust. Soc. Am*, vol. 88, pp. 1–37, 1978. [Online]. Available: http://dx.doi.org/10.1121/1.381962

[8] C. Jen, L. Piche, F. Bussiere. "Long isotropic buffer rods", *J. Acoust. Soc. Am*, vol. 88, pp. 23–25, 1990. [Online]. Available: http://dx.doi.org/10.1121/1.399946